Korean J. Chem. Eng., **28**(1), 79-83 (2011)
DOI: 10.1007/s11814-010-0335-z

Preparation, characterization, and oxidation catalysis of $H_3PMo_{12}O_{40}$ heteropolyacid catalyst immobilized on carbon aerogel

Yongju Bang*, Dong Ryul Park*, Yoon Jae Lee*, Ji Chul Jung, and In Kyu Song*,†**

*School of Chemical and Biological Engineering, Institute of Chemical Processes, Seoul National University, Shinlim-dong, Gwanak-gu, Seoul 151-744, Korea
**Department of Chemical Engineering, Myongji University, San 38-2, Nam-dong, Yongin, Gyeonggi-do 449-728, Korea
(*Received 5 March 2010 • accepted 28 May 2010*)

Abstract−Carbon aerogel (CA) with high surface area and large pore volume was prepared by polycondensation of resorcinol with formaldehyde. The surface of CA was then modified to have a positive charge, and thus to provide a site for the immobilization of $H_3PMo_{12}O_{40}$ (PMo_{12}) catalyst. By taking advantage of the overall negative charge of $[PMo_{12}O_{40}]^{3-}$, PMo_{12} catalyst was chemically immobilized on the surface-modified CA as a charge matching component. It was found that PMo_{12} catalyst was finely dispersed on the CA support via chemical interaction. In the vapor-phase 2-propanol conversion reaction, the PMo_{12}/CA catalyst showed a higher 2-propanol conversion than the unsupported PMo_{12} catalyst. Furthermore, the PMo_{12}/CA catalyst showed an enhanced oxidation catalytic activity (formation of acetone) and a suppressed acid catalytic activity (formation of propylene and isopropyl ether) compared to the unsupported PMo_{12} catalyst. The enhanced oxidation activity of PMo_{12}/CA catalyst was due to fine dispersion of $[PMo_{12}O_{40}]^{3-}$ on the CA support formed via chemical immobilization.

Key words: Heteropolyacid Catalyst, Carbon Aerogel, Chemical Immobilization, Oxidation Catalysis

INTRODUCTION

Heteropolyacids (HPAs) are early transition metal-oxygen anion clusters that have found successful applications in homogeneous and heterogeneous catalysis [1,2]. Among various HPA structural classes, the Keggin HPAs have been widely employed for acid-base and oxidation reactions [3,4]. One of the great advantages of HPA catalysts is that their catalytic properties can be tuned in a systematic way by changing the identity of counter-cations, heteroatoms, and framework polyatoms [5,6]. Another advantage that makes HPAs promising catalysts is their great thermal stability [7].

One of the disadvantages of HPA catalysts, however, is that their surface area is very low [8]. To overcome the low surface area, HPA catalysts have been conventionally supported on various inorganic materials such as silica [9], titania [10], and carbon [11]. Another promising approach for enlarging the surface area of HPA catalysts is to take advantage of the overall negative charge of heteropolyanions [12,13]. By this method, HPA catalysts have been immobilized on the positively charged supporting materials. However, such an attempt utilizing inorganic supporting materials has been restricted due to the difficulty in forming positive charge on the inorganic materials.

Among various inorganic supporting materials, carbon materials have been widely utilized in many areas due to their excellent thermal and mechanical stability [14,15]. Especially, carbon aerogels can be potentially available as supporting materials due to their high surface area, fine pore size, high porosity, non-toxicity, and availability [16]. These excellent properties of carbon aerogels are due to their three-dimensional mesoporous network of carbon nanoparticles [17]. If carbon aerogels are modified to have a positive charge for the immobilization of heteropolyanion, they can serve as an efficient support for HPA catalyst.

In this work, carbon aerogel (CA) with high surface area and large pore volume was prepared by polycondensation of resorcinol with formaldehyde. The surface of CA was then modified to have a positive charge, and thus to provide a site for the immobilization of $[PMo_{12}O_{40}]^{3-}$. $H_3PMo_{12}O_{40}$ (PMo_{12}) HPA catalyst was chemically immobilized on the surface-modified CA support as a charge matching component by taking advantage of the overall negative charge of $[PMo_{12}O_{40}]^{3-}$. The prepared PMo_{12}/CA catalyst was characterized by CHN, ICP-AES, FT-IR, FE-SEM, and XRD measurements. To examine the oxidation catalysis of PMo_{12}/CA catalyst, vapor-phase 2-propanol conversion reaction was carried out as a model reaction.

EXPERIMENTAL

1. Preparation of Carbon Aerogel

Carbon aerogel (CA) was prepared by polycondensation of resorcinol with formaldehyde in an aqueous solution. Sodium carbonate (Na_2CO_3, Sigma-Aldrich), which was used as a base catalyst, was mixed with resorcinol ($C_6H_6O_2$, Sigma-Aldrich) and deionized water to accelerate dehydrogenation of resorcinol. After the solution was stirred for a few minutes, formaldehyde (H_2CO, Sigma-Aldrich) was slowly added into the solution to form a sol. In this work, the molar ratio of resorcinol with respect to formaldehyde was fixed at 1 : 2, and the weight percentage of reactants in solution was about 40%. The molar ratio of resorcinol with respect to catalyst was fixed at 1,000. After the resulting sol was stirred, it was cured in a vial to form cylindrical shape at 80 °C for 2 days. Solvent exchange was performed with acetone at 50 °C for one day. Residual

†To whom correspondence should be addressed.
E-mail: inksong@snu.ac.kr

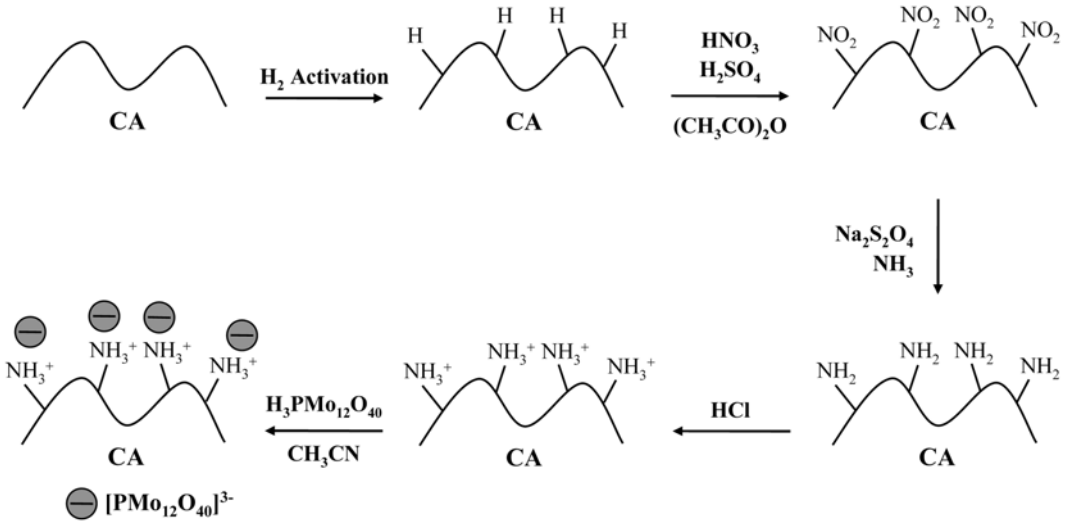

Fig. 1. Schematic procedures for the surface modification of carbon aerogel (CA) and the subsequent immobilization of $H_3PMo_{12}O_{40}$ (PMo_{12}) on the surface-modified carbon aerogel (CA).

solvent was replaced with fresh acetone every 3 h to remove water thoroughly from the pore of resorcinol-formaldehyde wet gel. Ambient drying was then done at room temperature and 50 °C for one day. Carbon aerogel (CA) was obtained by pyrolysis of resorcinol-formaldehyde aerogel at 800 °C for 2 h under nitrogen flow.

2. Surface Modification of CA and Immobilization of $H_3PMo_{12}O_{40}$ on the CA

Fig. 1 shows the schematic procedures for the surface modification of carbon aerogel (CA) and the subsequent immobilization of $H_3PMo_{12}O_{40}$ (PMo_{12}) on the surface-modified carbon aerogel (CA). CA was activated by flowing hydrogen at 200 °C, and then it was successively treated with acetic anhydride ($(CH_3CO)_2O$, Samchun), nitric acid (HNO_3, Samchun), and sulfuric acid (H_2SO_4, Sigma-Aldrich). The resulting nitrated CA was washed with de-ionized water and dried at 80 °C for 24 h. It was then treated with sodium hydrosulfite ($Na_2S_2O_4$, Samchun) dissolved in an ammonium hydroxide solution to form an amine group on the surface. The solid product was washed with de-ionized water and dried at 80 °C for 24 h to yield the surface-modified CA. The surface-modified CA (0.85 g) was reacted with $H_3PMo_{12}O_{40}$ (PMo_{12}) (0.85 g, Sigma-Aldrich) dissolved in 50 ml of acetonitrile (CH_3CN, Sigma-Aldrich) for the immobilization of PMo_{12} on the surface-modified CA. The resulting solid product was washed with de-ionized water several times, until the washing solvent became colorless. It was finally dried at 80 °C for 24 h to yield the PMo_{12}/CA.

3. Characterization

Surface areas and pore volumes of CA, surface-modified CA, and PMo_{12}/CA catalyst were obtained with an ASAP-2010 instrument (Micromeritics). To ensure the successful surface modification of CA support, nitrogen contents of surface-modified CA and PMo_{12}/CA were measured by CHN elemental analyses (Leco, CHNS-932). PMo_{12} content in the PMo_{12}/CA was measured by ICP-AES analyses (Perkin Elmer, Optima-4300 DV). FT-IR spectra were obtained with a Nicolet 6700 FT-IR spectrometer. Surface morphologies of CA and PMo_{12}/CA were examined by FE-SEM analyses (Jeol, JSM-6700F). Crystalline phases of unsupported PMo_{12}, CA, and PMo_{12}/CA were examined by XRD measurements (Mac Science, M18XHF-SRA).

4. Vapor-phase 2-Propanol Conversion Reaction

Vapor-phase 2-propanol conversion reaction was carried out in a continuous flow fixed-bed reactor at atmospheric pressure. Unsupported PMo_{12} (20 mg) or PMo_{12}/CA (20 mg on PMo_{12} basis) was charged into a tubular quartz reactor, and then it was pretreated with a mixed stream of nitrogen (20 ml/min) and oxygen (5 ml/min) at 240 °C for 1 h. 2-Propanol (3.9×10^{-3} mol/h) was sufficiently vaporized by passing through a pre-heating zone and was continuously fed into the reactor together with a mixed stream of nitrogen (20 ml/min) and oxygen (5 ml/min). The catalytic reaction was carried out at 220 °C for 5 h. Reaction products were periodically sampled and analyzed with a gas chromatograph (HP 5890II). Conversion of 2-propanol and selectivity for product (acetone, propylene, and isopropyl ether) were calculated on the basis of carbon mole balance.

RESULTS AND DISCUSSION

1. Physicochemical Properties of CA, Surface-modified CA, and PMo_{12}/CA

Fig. 2 shows the nitrogen adsorption-desorption isotherms of CA and PMo_{12}/CA. It was clearly observed that both CA support and PMo_{12}/CA catalyst exhibited type IV isotherm with H2 type hysteresis loop, indicating the existence of well-developed porous structure. Characterization results for CA, surface-modified CA, and PMo_{12}/CA are summarized in Table 1. BET surface areas and pore volumes decreased in the order of CA>surface-modified CA>PMo_{12}/CA. Surface area of CA decreased after the surface modification step due to the formation of amine functional groups on the surface of CA. PMo_{12}/CA catalyst also showed a lower surface area than the surface-modified CA support due to the immobilization of PMo_{12} catalyst. However, PMo_{12}/CA catalyst still retained high surface area (549 m^2/g) and large pore volume (1.49 cm^3/g). These results indicate that pore structure of CA was still maintained even after

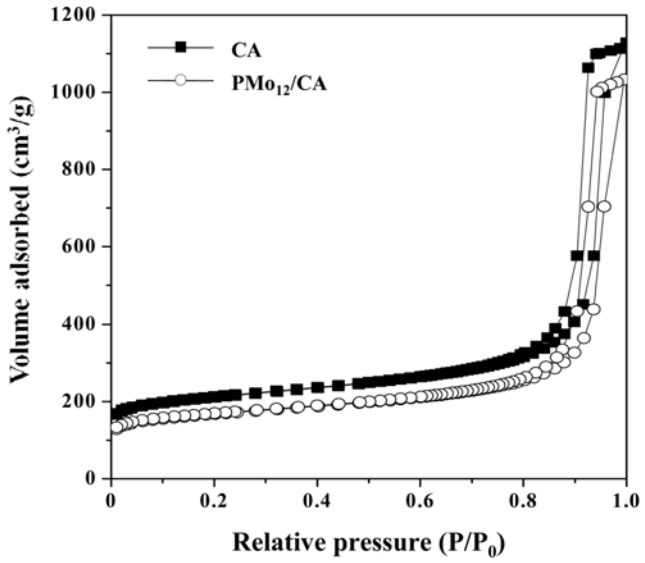

Fig. 2. Nitrogen adsorption-desorption isotherms of CA and PMo_{12}/CA.

Table 1. Characterization results for CA, surface-modified CA, and PMo_{12}/CA

	Nitrogen content (wt%)	PMo_{12} content (wt%)	BET surface area (m^2/g)	Pore volume (cm^3/g)
CA	-	-	689	1.58
Surface-modified CA	1.1	-	597	1.51
PMo_{12}/CA	0.9	3.0	549	1.49

the immobilization of PMo_{12}.

The nitrogen content of surface-modified CA and PMo_{12}/CA was measured by CHN elemental analyses. No nitrogen was detected in the bare CA sample. The nitrogen content of surface-modified CA and PMo_{12}/CA was 1.1 wt% and 0.9 wt%, respectively. This indicates that amine functional groups were successfully formed on the CA via surface modification step. The decreased nitrogen content of PMo_{12}/CA catalyst was due to the loading of PMo_{12}. The amount of PMo_{12} catalyst immobilized on CA was measured to be 3.0 wt%. It should be noted that PMo_{12} catalyst physically supported on CA was totally dissolved out during the washing step. This implies that nitrogen in the surface-modified CA played a key role in forming a nitrogen-derived functional group (amine group) for the immobilization of PMo_{12}.

2. Chemical Immobilization of PMo_{12} Catalyst on the CA Support

Chemical immobilization of PMo_{12} catalyst on the CA support was confirmed by FT-IR analyses. FT-IR spectra of unsupported PMo_{12}, CA, and PMo_{12}/CA are shown in Fig. 3. The primary structure of PMo_{12} catalyst could be identified by four characteristic IR bands appearing in the range of 700-1,200 cm^{-1} [8,18]. The four characteristic IR bands of unsupported PMo_{12} appeared at 1,064 cm^{-1} (P-O), 962 cm^{-1} (Mo=O), 866 cm^{-1} (interoctahedral Mo-O-Mo), and 789 cm^{-1} (intraoctahedral Mo-O-Mo). However, CA showed no characteristic IR bands in the range of 700-1,200 cm^{-1} because

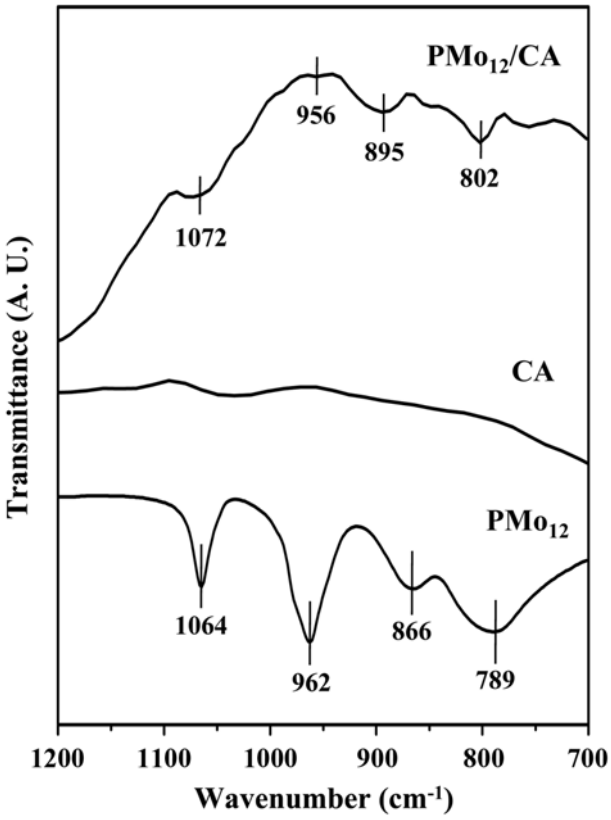

Fig. 3. FT-IR spectra of unsupported PMo_{12}, CA, and PMo_{12}/CA.

of the strong absorbance of carbon material by infrared beam. The characteristic IR bands of PMo_{12}/CA catalyst were observed at 1,072 cm^{-1}, 956 cm^{-1}, 895 cm^{-1}, and 802 cm^{-1} for P-O, Mo=O, interoctahedral Mo-O-Mo, and intraoctahedral Mo-O-Mo bands, respectively. It is noteworthy that the characteristic IR bands of PMo_{12} in the PMo_{12}/CA appeared at shifted positions compared to those of unsupported PMo_{12}. This result means that PMo_{12} was successfully immobilized on the CA support via strong chemical interaction between PMo_{12} and CA support.

3. Fine Dispersion of PMo_{12} Catalyst on the CA Support

Fig. 4 shows the FE-SEM images of CA and PMo_{12}/CA. It was observed that CA with high surface area and well developed interparticular porous structure was successfully prepared by polycondensation of resorcinol with formaldehyde. It should be noted that there was no significant difference in surface morphology between CA and PMo_{12}/CA. This indicates that CA was morphologically stable even after the surface modification step and the subsequent immobilization step of PMo_{12}. Furthermore, no visible evidence representing PMo_{12} agglomerates was found in the FE-SEM image of PMo_{12}/CA, indicating that PMo_{12} catalyst was finely dispersed on the surface of CA.

Fig. 5 shows the XRD patterns of unsupported PMo_{12}, CA, and PMo_{12}/CA. Unsupported PMo_{12} catalyst showed the characteristic XRD pattern of the HPA catalyst. On the other hand, CA support exhibited two broad peaks at 2θ=23.5° and 43.8°, which were attributed to a graphitic-like structure [19]. The PMo_{12}/CA catalyst showed no characteristic peaks of HPA but exhibited almost the same XRD pattern as CA support, even though PMo_{12} was loaded in the PMo_{12}/

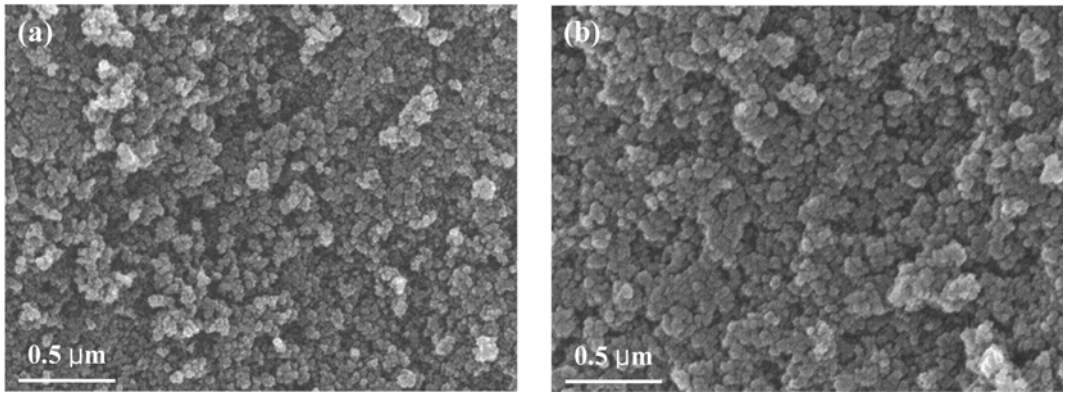

Fig. 4. FE-SEM images of (a) CA and (b) PMo_{12}/CA.

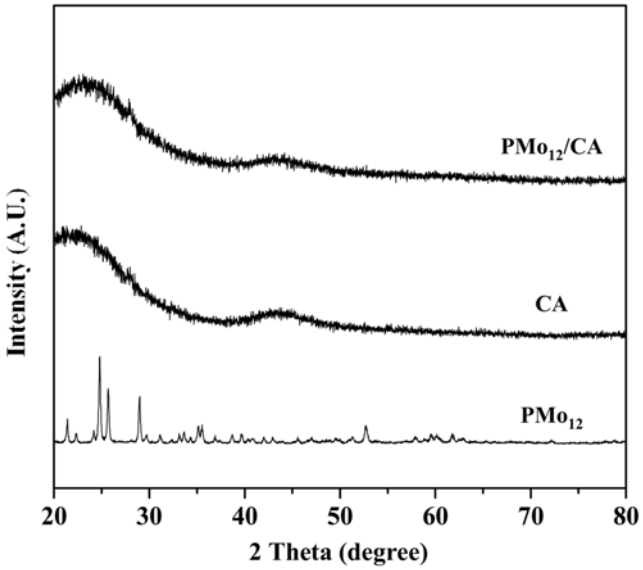

Fig. 5. XRD patterns of unsupported PMo_{12}, CA, and PMo_{12}/CA.

CA catalyst. This result indicates that PMo_{12} catalyst was finely and molecularly dispersed on the CA support. Thus, the amine functional group on the surface-modified CA efficiently served as an anchoring site for the chemical immobilization of $[PMo_{12}O_{40}]^{3-}$.

4. Oxidation Catalysis of PMo_{12}/CA in the Vapor-phase 2-Propanol Conversion Reaction

To examine the catalytic performance of unsupported PMo_{12} and PMo_{12}/CA catalysts, vapor-phase 2-propanol conversion reaction was carried out as a model reaction. In the catalytic reaction, acetone was formed by the oxidation catalytic function of HPA, while propylene and isopropyl ether were produced by the acid catalytic function of HPA [20]. Fig. 6 shows the typical catalytic performance of PMo_{12}/CA in the vapor-phase 2-propanol conversion reaction with time on stream at 220 °C. The PMo_{12}/CA catalyst showed a stable catalytic performance during the reaction. The unsupported PMo_{12} catalyst also showed a stable catalytic performance with time on stream.

Fig. 7 shows the steady-state catalytic performance of unsupported PMo_{12} and PMo_{12}/CA catalysts in the vapor-phase 2-propanol conversion reaction after a 5-h reaction. The PMo_{12}/CA catalyst showed a higher 2-propanol conversion than the unsupported PMo_{12} cata-

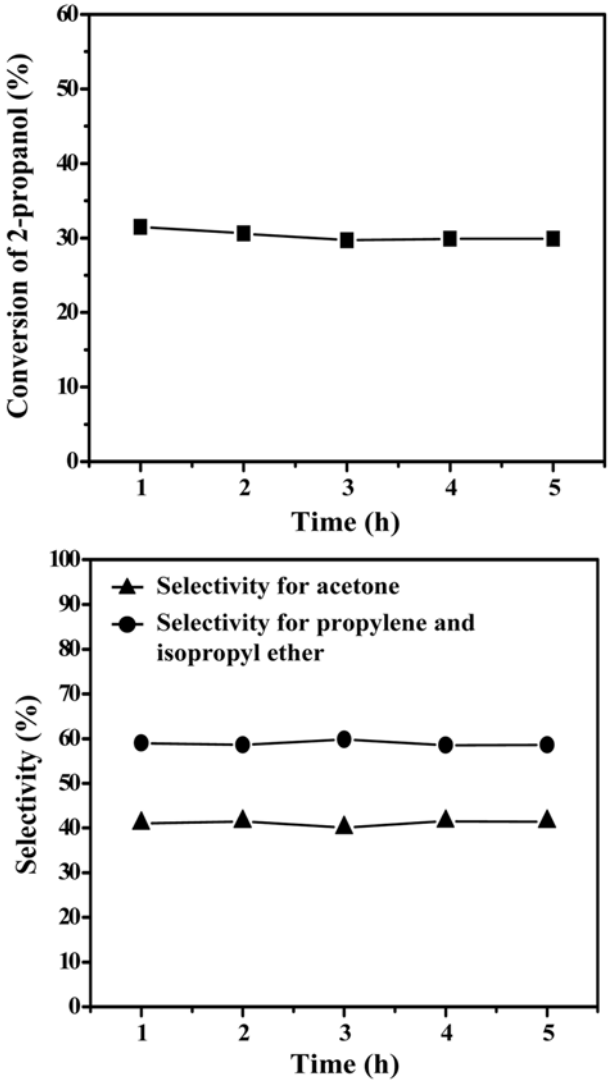

Fig. 6. Typical catalytic performance of PMo_{12}/CA in the vapor-phase 2-propanol conversion reaction with time on stream at 220 °C.

lyst. The enhanced 2-propanol conversion of PMo_{12}/CA was attributed to fine dispersion of PMo_{12} species on the CA support formed via chemical immobilization. Furthermore, the PMo_{12}/CA catalyst

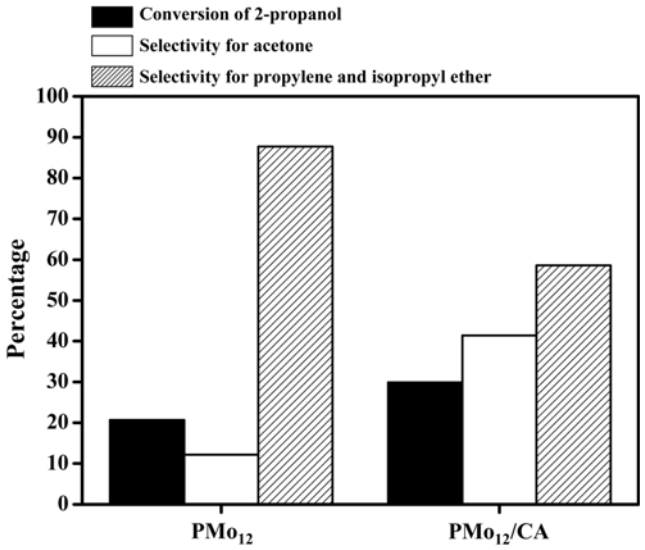

Fig. 7. Steady-state catalytic performance of unsupported PMo_{12} and PMo_{12}/CA catalysts in the vapor-phase 2-propanol conversion reaction after a 5-h reaction.

showed enhanced oxidation catalytic activity (formation of acetone) and suppressed acid catalytic activity (formation of propylene and isopropyl ether) compared to the unsupported PMo_{12} catalyst. The unsupported PMo_{12} catalyst retains its own acid and oxidation function. In the PMo_{12}/CA catalyst, however, $[PMo_{12}O_{40}]^{3-}$ was chemically and molecularly immobilized on the CA support as a charge matching component by losing its proton (Brönsted acid site). Therefore, the PMo_{12}/CA catalyst exhibited a better oxidation catalytic activity and a lower acid catalytic activity than the unsupported PMo_{12} catalyst. It is concluded that the PMo_{12}/CA served as an efficient oxidation catalyst in this model reaction.

CONCLUSIONS

Carbon aerogel (CA) with high surface area (689 m^2/g) and large pore volume (1.58 cm^3/g) was prepared by polycondensation of resorcinol with formaldehyde. $H_3PMo_{12}O_{40}$ (PMo_{12}) catalyst was successfully immobilized on the CA support by taking advantage of the overall negative charge of $[PMo_{12}O_{40}]^{3-}$. The amine functional group formed on the surface-modified CA played an important role for the immobilization of PMo_{12}. PMo_{12}/CA catalyst still retained high surface area (549 m^2/g) and large pore volume (1.49 cm^3/g), indicating that the pore structure of CA support was still maintained even after the immobilization of PMo_{12}. It was also found that PMo_{12} was finely dispersed on the CA support via chemical interaction. In the vapor-phase 2-propanol conversion reaction, the PMo_{12}/CA catalyst showed a higher 2-propanol conversion than the unsupported PMo_{12} catalyst due to finely and molecularly dispersed PMo_{12} species on the CA support. Furthermore, the PMo_{12}/CA catalyst showed enhanced oxidation catalytic activity (formation of acetone) and suppressed acid catalytic activity (formation of propylene and isopropyl ether) compared to the unsupported PMo_{12} catalyst. The enhanced oxidation activity of PMo_{12}/CA catalyst was attributed to fine dispersion of $[PMo_{12}O_{40}]^{3-}$ on the CA support, where PMo_{12} was chemically immobilized on the positive site of surface-modified CA support by sacrificing its proton (Brönsted acid site). Thus, the PMo_{12}/CA catalyst served as an efficient oxidation catalyst in the 2-propanol conversion reaction.

ACKNOWLEDGEMENTS

This work was supported by the National Research Foundation of Korea (NRF) grant funded by the Korea government (MEST) (No. 2010-0000301).

REFERENCES

1. C. L. Hill and C. M. Prosser-McCartha, *Coord. Chem. Rev.*, **143**, 407 (1995).
2. M. Misono, *Catal. Rev. Sci. Eng.*, **29**, 269 (1987).
3. I. V. Kozhevnikov, *Catal. Rev. Sci. Eng.*, **37**, 311 (1995).
4. N. Mizuno and M. Misono, *Chem. Rev.*, **98**, 199 (1998).
5. I. K. Song and M. A. Barteau, *Korean J. Chem. Eng.*, **19**, 567 (2002).
6. M. H. Youn, D. R. Park, J. C. Jung, H. Kim, M. A. Barteau and I. K. Song, *Korean J. Chem. Eng.*, **24**, 51 (2007).
7. M. T. Pope, *Heteropoly and isopoly oxometalates*, Springer-Verlag, New York (1983).
8. T. Okuhara, N. Mizuno and M. Misono, *Adv. Catal.*, **41**, 113 (1996).
9. N.-Y. He, C.-S. Woo, H.-G. Kim and H.-I. Lee, *Appl. Catal. A*, **281**, 167 (2005).
10. J. PoŸniczek, A. Lubañska, A. Micek-Ilnicka, D. Mucha, E. Lalik and A. Bilañski, *Appl. Catal. A*, **298**, 217 (2006).
11. F. X. Liu-Cai, B. Sahut, E. Faydi, A. Auroux and G. Herve, *Appl. Catal. A*, **185**, 75 (1999).
12. M. Hasik, W. Turek, E. Stochmal, M. Lapowski and A. Proñ, *J. Catal.*, **147**, 544 (1994).
13. H. Kim, P. Kim, K.-Y. Lee, S. H. Yeom, J. Yi and I. K. Song, *Catal. Today*, **111**, 361 (2006).
14. Q. Wang, H. Li, L. Chem and X. Huang, *Carbon*, **39**, 2211 (2001).
15. J. L. Zimmerman, R. Williams, V. N. Khabashesku and J. L. Margrave, *Nano Lett.*, **1**, 731 (2001).
16. A. C. Pierre and G. M. Pajonk, *Chem. Rev.*, **102**, 4243 (2002).
17. R. W. Pekala, *J. Mater. Sci.*, **24**, 3221 (1989).
18. J. F. Keggin, *Nature*, **131**, 908 (1933).
19. Z. Q. Li, C. J. Lu, Z. P. Xia, Y. Zhou and Z. Luo, *Carbon*, **45**, 1686 (2007).
20. J. K. Lee, I. K. Song, W. Y. Lee and J.-J. Kim, *J. Mol. Catal. A*, **104**, 311 (1996).